ANL/CMT/CP - 97942

# Corrosion Testing of Stainless Steel-Zirconium Metal Waste Form

By

Daniel P. Abraham
Argonne National Laboratory
Chemical Technology Division
9700 S. Cass Ave.
Argonne, IL 60439
Phone: (630) 252-4332
Fax: (630) 252-9917
e-mail: abraham@cmt.anl.gov



To be published in the proceedings for the 1998 Fall MRS Meeting
Boston, MA
Nov. 29-Dec. 4, 1998

## DISCLAIMER

# CORROSION TESTING OF STAINLESS STEEL–ZIRCONIUM METAL WASTE FORMS

Daniel P. Abraham, Lin J. Simpson, Michele J. DeVries, and Sean M. McDeavitt
Chemical Technology Division, Argonne National Laboratory, Argonne, IL 60439

## ABSTRACT

Stainless steel–zirconium (SS–Zr) alloys are being considered as waste forms for the disposition of metallic waste generated during the electrometallurgical treatment of spent nuclear fuel. The waste forms contain irradiated cladding hulls, components of the alloy fuel, noble metal fission products, and actinide elements. The baseline waste form is a stainless steel–15 wt% zirconium (SS–15Zr) alloy. This article presents microstructures and some of the corrosion studies being conducted on the waste form alloys. Electrochemical corrosion, immersion corrosion, and vapor hydration tests have been performed on various alloy compositions to evaluate corrosion behavior and resistance to selective leaching of simulated fission products. The SS–Zr waste forms are successful at the immobilization and retention of fission products and show potential for acceptance as high–level nuclear waste forms.

## 1.0 INTRODUCTION

Stainless steel–zirconium alloys have been developed for the disposition of metallic waste, generated during the electrometallurgical treatment of spent nuclear fuel, from the Experimental Breeder Reactor–II (EBR–II) located at the Argonne National Laboratory site in Idaho (ANL–W) [1, 2]. In the electrometallurgical process, chopped driver or blanket fuel segments are placed into the anode baskets of an electrorefiner. When a potential is applied, uranium, active fission products, and transuranic elements dissolve at the anode into the molten salt electrolyte, while uranium is deposited onto a steel cathode [3].

The irradiated fuel cladding, assembly hardware, zirconium from the alloy fuel, noble metal[1] fission products (NMFP) (e.g., Tc, Rh, Ru, Pd, and Nb), and remnant actinides left behind in the anodic dissolution baskets are melted together to make a metal waste form (MWF) intended for disposal in a geologic repository. The baseline waste form for EBR–II spent fuels is the stainless steel–15 wt% zirconium (SS–15Zr) alloy [1, 2]. However, the zirconium content of MWF alloys may vary from 5 to 20 wt% Zr depending on the composition of the starting fuel. The noble metal content of the waste forms also depend on the burnup of the treated fuel and the actinide content on the efficiency of the electrorefining process; the waste forms may contain up to 4 wt% NMFP and up to 10 wt% actinides (mainly uranium).

This article briefly describes the microstructures and some of the corrosion studies being conducted on representative, but nonradioactive, MWF alloys. Electrochemical corrosion measurements have been conducted at various solution pH values to obtain relative values of corrosion rate for the various MWF alloy compositions. Immersion tests in deionized water and in simulated J–13 groundwater (representative of the proposed Yucca Mountain geologic

[1] The term "noble metal" means a metallic element that is inert or electrochemically noble during the electrometallurgical process.

repository in Nevada) have been performed to evaluate the release of elements (especially fission products) from the alloys. Tests in a saturated steam environment have been conducted to determine the nature and thickness of corrosion layers that form on the metallic alloys. Corrosion tests on actual radioactive waste forms arising from the treatment of EBR–II fuels will be presented in future articles.

## 2.0 MICROSTRUCTURES OF THE METAL WASTE FORM ALLOY

Stainless steel–zirconium alloy ingots were prepared from Type 316 stainless steel (SS316), high–purity zirconium, and representative noble metal elements. The alloys were prepared as small–scale samples (20–40 g) in a resistance–heated furnace and as larger samples (~ 2.5 kg) in an induction casting furnace. The starting materials were contained in yttrium oxide crucibles and heated to 1600°C under high–purity argon for ~1 to 2 h. All ingots were produced by allowing the melt to solidify within the yttrium oxide crucibles. The phases in various alloy ingots were identified by using a combination of scanning electron microscopy (SEM) and diffraction (X–ray and neutron) techniques.

Zirconium has very low solubility in iron. The addition of zirconium to SS316 results in the formation of $ZrFe_2$–type Laves and other intermetallic phases; the amount of these phases depends on the zirconium content of the alloy. For example, the intermetallic content of a stainless steel–5 wt% Zr (SS–5Zr) alloy (see Fig. 1a) is ~10 vol%, and that of a stainless steel–15 wt% Zr (SS–15Zr) alloy is ~50 vol% (see Fig. 1b). The intermetallic phases are strong sinks for the austenite stabilizer, nickel. Intermetallic formation leads to nickel consumption from the austenite ($\gamma$) phase and, consequently, to austenite destabilization and ferrite ($\alpha$) formation. Figure 1a shows that ferrite, austenite, and $Zr(Fe,Cr,Ni)_{2+x}$ are the major phases in SS–5Zr, whereas only ferrite and $Zr(Fe,Cr,Ni)_{2+x}$ are prominent in SS–15Zr.

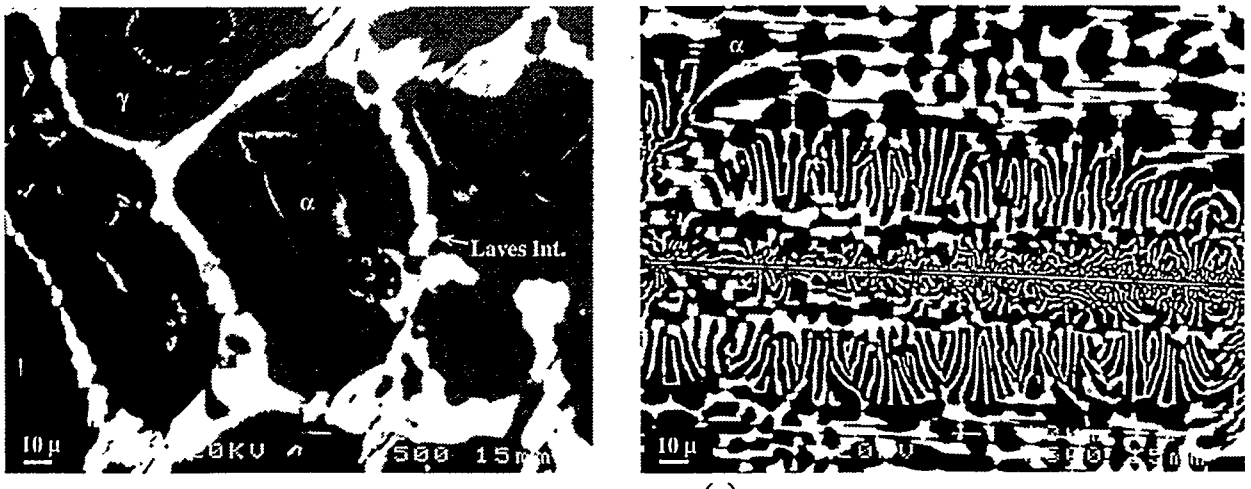


(a)

Fig.1. (a) Typical microstructure in a stainless steel–5 wt% Zr alloy. The dark phase is $\alpha$ (ferrite), the gray phase is $\gamma$ (austenite) and the bright regions are $Zr(Fe,Cr,Ni)_{2+x}$. (b) Typical microstructure in a stainless steel–15 wt% Zr alloy. The dark regions are ferrite and the bright regions are $ZrFe_2$–type intermetallics.

The phases observed in the microstructure of SS–Zr alloys are summarized in Table 1. The intermetallic phases are the "preferred" location for several noble metal elements. Fission product incorporation in SS–Zr alloy phases is strongly influenced by the volume fraction of the intermetallics, which is, in turn, influenced by the zirconium content of the waste form. The noble metals form discrete phases in a stainless steel alloy without Zr; this SS316 composition is not being considered as a waste form. Noble metal–rich phases are rarely observed in SS–Zr alloys with > 5 wt% Zr. The noble metal elements are dissolved in the major phases of the SS–15Zr and the stainless steel–20 wt% Zr (SS–20Zr) alloy. Niobium–rich areas are occasionally observed at the austenite–ferrite interfaces of SS–5Zr alloys containing this element.

Table 1. Phases Observed in the Microstructure of Stainless Steel– Zirconium Alloys

| Alloy Composition | Phases | |
|---|---|---|
| | Major | Minor |
| SS316 | $\gamma$ | – |
| SS–5Zr | $\gamma + \alpha + Zr(Fe,Cr,Ni)_{2+x}$ | – |
| SS–5Zr–2Nb–1Pd–1Ru | $\gamma + \alpha + Zr(Fe,Cr,Ni)_{2+x}$ | Nb–rich regions at $\gamma/\alpha$ interface |
| SS–15Zr | $\alpha + Zr(Fe,Cr,Ni)_{2+x}$ | $\gamma$, Fe23Zr6–type intermetallic |
| SS–15Zr–1Nb–1Pd–1Rh–1Ru | $\alpha + Zr(Fe,Cr,Ni)_{2+x}$ | $\gamma$, Fe23Zr6–type intermetallic |
| SS–20Zr–2Nb–1Pd–1Ru | $\alpha + Zr(Fe,Cr,Ni)_{2+x}$ | – |

$\gamma$ = Austenite, $\alpha$ = Ferrite, $Zr(Fe,Cr,Ni)_{2+x}$ = $ZrFe_2$–type Laves intermetallic phase

## 3.0 CORROSION BEHAVIOR

### 3.1 Electrochemical Corrosion Testing

The polarization resistance technique [5] based on ASTM G59 was used to study the *relative* corrosion behavior of the various SS-Zr alloy compositions. The measurements were conducted in a corrosion cell consisting of a round-bottomed flask, graphite auxiliary electrodes, and a standard calomel electrode which served as the reference electrode. The applied potential and resulting current were measured by a Versastat–II Potentiostat/Galvanostat and with SoftCorr III Corrosion Measurement software from EG&G Instruments.

Corrosion rates were measured in test solutions that ranged in pH from 2 to 10. The pH of our simulated J–13 composition was ~9; the acid and base solutions were prepared by adding hydrochloric acid and sodium hydroxide, respectively, to the J–13 composition. The pH=2 solution represents an extreme condition that may not occur naturally in the repository environment, but is included as an aggressive test for the alloy samples.

Disk specimens (16-mm dia. and 3-mm. thk.) were polished to a 600 grit finish and immersed in the test solutions. After equilibration for more than 0.5 hour, the sample potential was scanned ±20 mV about the corrosion potential at a rate of 0.6 V/h (0.166 mV/s). The slope of the potential–current curve yielded the polarization resistance. The corrosion currents calculated from the polarization resistance (assuming anodic and cathodic Tafel constants to be 0.1 V) were converted into corrosion rates and are presented graphically in Fig. 2.

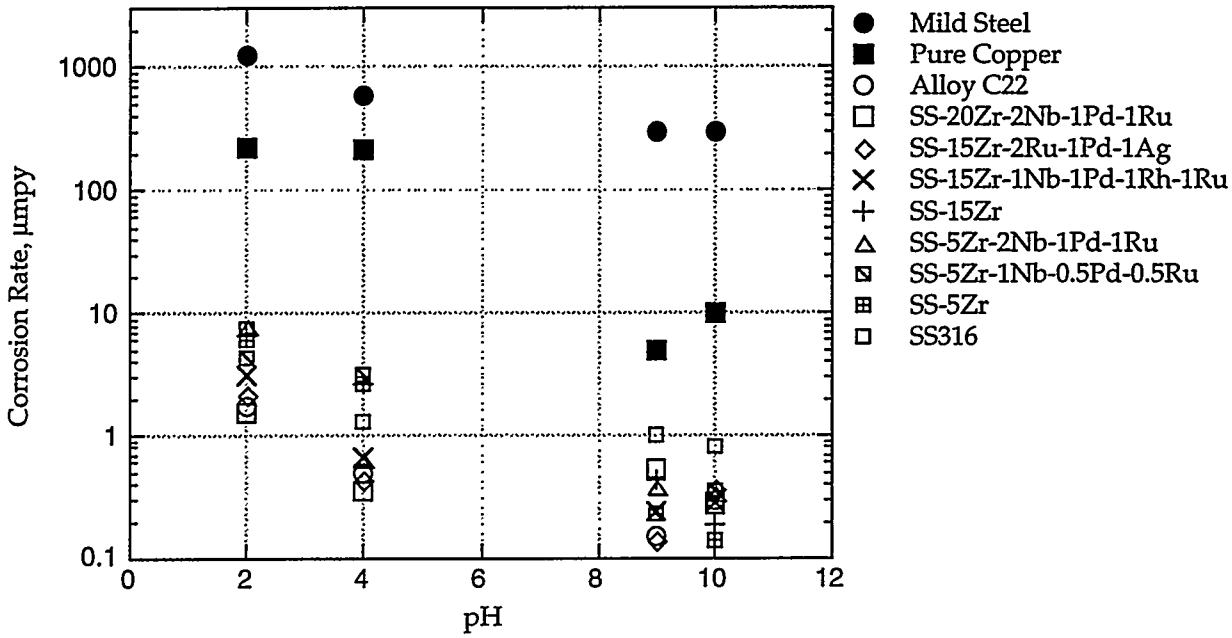


Fig. 2. Graphical representation of corrosion rates measured for various alloys (µmpy= microns per year).

It is obvious that the corrosion rates for the various SS–Zr alloy samples are similar; the rates are not affected by additions of noble metal elements. In general, the corrosion rates in simulated J–13 solution (pH = 9) and pH = 10 solutions are comparable. The corrosion rates in the acidic solutions are higher; for most stainless steel– zirconium samples, the rates in pH = 2 solution are at least an order of magnitude larger than the rates in pH = 10 solution.

The corrosion rates for the stainless steel– zirconium alloys are one to two orders of magnitude lower than the rate for pure copper, and two to three orders of magnitude lower than the rate for mild steel. They are also comparable in magnitude to those for 316 stainless steel and Alloy C22, alloys that have been evaluated as candidates for nuclear waste canisters [6]. The results of electrochemical testing demonstrate that stainless steel–zirconium alloys are suitable for disposal of nuclear waste in a geologic repository.

## 3.2 Immersion Testing

Immersion tests provide information on the selective leaching of elements into representative test solutions. Our test procedure was based on MCC–1 (ASTM C 1220) and involved exposing the sample to a static solution for an extended duration at a fixed temperature. The outcome of the test was evaluated by measuring changes in specimen mass and solution composition and by examining the specimen surface for qualitative corrosion information.

Immersion tests at 90°C in simulated J–13 solution[2] were conducted on MWF samples of various compositions for durations up to 10,000 h (417 d). Disk–shaped specimens were polished to a 240 grit finish, then immersed in the test solution in sealed Teflon vessels. Minimal surface corrosion was observed on the test specimens even after 10,000 h; most samples

[2] A representative composition of J–13 well water is (in mg/L): 11.5 Ca, 1.76 Mg, 45.0 Na, 5.3 K, 0.06 Li, 0.04 Fe, 0.001 Mn, 0.03 Al, 30.0 Si, 2.1 $F^-$, 6.4 $Cl^-$, 18.1 $SO_4^{2-}$, 10.1 $NO_3^-$, and 143.0 $HCO_3^-$ [7].

retained their as–polished surfaces. The weight changes observed were very small and often within the resolution limit of the balance (±0.0001 g). Negligible quantities of alloy constituents were present in the test solution, clearly indicating that the alloy samples were very corrosion resistant.

Immersion tests at 200°C were conducted to accelerate alloy corrosion and increase elemental dissolution into test solutions. Alloy disk specimens, 10-mm dia. and 2-mm thk., polished to a 240 grit finish were immersed in deionized water and sealed in titanium vessels for 28 days. The sample surfaces were examined after test completion, and a brief description of the surface appearance is reported in Table 2. All specimens exhibited some degree of surface corrosion. The specimens containing 15 wt% Zr and 20 wt% Zr showed uniform corrosion, whereas the 5 wt% Zr specimens showed localized attack. The weight changes for the samples were small and within ± 0.0001 g.

The test solutions were analyzed for the presence of elemental constituents from the alloys. The elements sorbed on the walls of the test vessel were removed by 1 wt% nitric acid; this "acid strip" solution was also analyzed. The elemental concentrations were obtained either by inductively coupled plasma-mass spectroscopy or inductively coupled plasma-atomic emission spectroscopy. The results showed that (1) elements such as Zr and Nb are often present in amounts below the detectability limits of the measuring instruments and (2) elements including Fe, Pd, Rh, Ru, and Mo may not be present in the test solutions but are often present in the acid strip solutions, i.e., they plate out on the test vessel walls.

The normalized elemental losses for the various alloy compositions studied are shown in Table 2; the data represents average values obtained from testing multiple specimens. Of the major alloying elements, Ni leaches out the most followed by Cr, Mn and Fe; the highest loss (1.1 $g/m^2$) was observed for Ni in the SS–5Zr–2Nb–1Ru–1Pd alloy. The noble metal fission product elements show much smaller losses; the highest loss was observed for Mo (0.09 $g/m^2$) in the SS–20Zr–2Nb–1Ru–1Pd alloy. It is evident that all alloy compositions considered in our study display similar corrosion resistance and, more importantly, excellent retention of fission product elements.

Table 2. Results of Visual Examination and Normalized Loss (NL) (average values obtained from multiple specimens) for MWF Specimens Immersed in 200°C Deionized Water for 28 Days (S/V = 10 $m^{-1}$)

| Alloy Composition | Visual Examination of Sample Surface | NL (Major Elements), $g/m^2$ | | | | | NL (NMFP), $g/m^2$ | | | | |
|---|---|---|---|---|---|---|---|---|---|---|---|
| | | Fe | Cr | Ni | Zr | Mn | Mo | Nb | Pd | Rh | Ru |
| SS-5Zr-1Nb-0.5Ru-0.5Pd | Localized corrosion; intermetallic network etched out | [a] | 0.035 | 0.33 | [a] | 0.056 | 0.02 | [a] | 0.006 | [b] | 0.0008 |
| SS-5Zr-2Nb-1Ru-1Pd | Localized corrosion; intermetallic network etched out | 0.014 | 0.53 | 1.13 | [a] | 0.21 | 0.087 | 0.004 | 0.0039 | [b] | 0.0018 |
| SS-15Zr-1Nb-1Ru-1Pd-1Rh | Mostly brown; uniform corrosion | 0.47 | 0.073 | 0.58 | [a] | 0.067 | 0.022 | [a] | 0.0047 | 0.0005 | 0.0006 |
| SS-20Zr-2Nb-1Ru-1Pd | Mostly dark brown; uniform corrosion | 0.0002 | 0.13 | 0.66 | [a] | 0.055 | 0.092 | [a] | 0.013 | [b] | 0.0021 |

[a]Element below detectability limits of measuring instrument [b]Element not present in alloy

3.3 Steam Corrosion (Vapor Hydration) Testing

The vapor hydration test, an accelerated test developed to measure the durability of glass waste forms [8], was used to study the corrosion behavior of the MWF alloys. In this test, monolith specimens are suspended in a sealed stainless steel vessel containing a small pool of deionized water beneath the specimen. The water vaporizes and creates a saturated steam environment when the sealed vessel is heated to 200°C. The metallic specimens were tested for extended durations under these conditions, and corrosion behavior was measured as a function of (1) corrosion layer thickness and (2) nature of the corrosion products formed on sample surfaces.

Table 3 summarizes tests results on pure iron, copper, 316 stainless steel, SS–15Zr, and SS–15Zr–2Ru–1.5Pd–0.5Ag. The oxide type was revealed by a combination of techniques including scanning electron microscopy, X-ray diffraction and Raman spectroscopy. The pure iron specimens showed the most corrosion; a porous, nonuniform oxide layer, ~10–60 μm thick, formed within 7 days. The oxide layer thickness did not increase appreciably after this time period, suggesting limited oxygen availability after 7 days. The oxide layers contained hematite ($Fe_2O_3$), magnetite ($Fe_3O_4$), and FeO. The oxide layer that formed on the surfaces of Cu specimens was relatively uniform and increased slowly with time. The average thickness of the oxide layer increased from ~3 μm after 7 days to ~12 μm after 182 days. The copper oxide layers contained both cuprite ($Cu_2O$) and tanorite (CuO).

Table 3. Oxide Layers Formed on Various Metallic Samples in Steam at 200°C

| Sample Composition | Test Period, days | Oxide Thickness, mm | Oxide Type |
|---|---|---|---|
| Pure Fe | 3 | ~2–6 | $Fe_2O_3$, $Fe_3O_4$, FeO |
| | 7 | ~10–60 | |
| | 28 | ~10–80 | |
| | 56 | ~10–60 | |
| | 182 | ~10–60 | |
| Pure Copper | 7 | ~1–5 | CuO, $Cu_2O$ |
| | 56 | ~5–10 | |
| | 182 | ~5–20 | |
| SS316 | 56 | ~0–2 | $Fe_2O_3$, $Fe_3O_4$, |
| | 182 | ~1–3 | $FeNiCrO_4$ |
| SS-15Zr | 56 | ~0–2 | $Fe_2O_3$, $Fe_3O_4$, |
| | 182 | ~1–3 | $FeNiCrO_4$ |
| SS304-15Zr-2Ru-1.5Pd-0.5Ag | 56 | ~0–2 | Not Determined |

In contrast, the oxide layers formed on type 316 stainless steel and the SS–15Zr specimens were small and averaged ~1 μm for the 56-day and 182-day tests. The thin corrosion layers made oxide identification difficult; Raman spectroscopy results suggested the presence of $Fe_2O_3$, $Fe_3O_4$, and $FeCrNiO_4$ in the corrosion products. Sufficient oxygen was available in the sealed vessels to support oxide growth beyond the ~1 μm oxide layer observed on the stainless steel and SS–15Zr specimens. The protective oxide layers that form on the stainless steel and SS–15Zr alloys apparently impede oxygen diffusion and retard further oxide growth (passivation behavior).

Under similar testing conditions, some borosilicate glasses and other ceramic–based waste forms show alteration layers that are up to 300–μm thick [8, 9]. The environmental assessment (EA) glass, used for comparisons when qualifying glass waste forms for disposal, was completely converted to a crystalline powder after only 3 days in vapor hydration tests at 200°C. Other representative glass waste forms (e.g., SRL–165 and SRL–202) exhibit relatively high durability, with alteration layers having thicknesses between 50 and 200 μm after 56 days at 200°C [9]. The relatively small oxide layers that form on the stainless steel– zirconium alloys demonstrate the excellent durability of these waste forms.

## 4.0 SUMMARY

Stainless steel– zirconium waste form alloys are very resistant to the normal corrosion conditions envisioned at the proposed Yucca Mountain geologic repository. Electrochemical corrosion tests have indicated that the corrosion resistance of the alloys is comparable to that of 316 stainless steel and Alloy C22. Immersion tests at 90°C in simulated J–13 solution and at 200°C in deionized water have shown that the selective leaching of fission products from the alloy samples is very small. Corrosion tests in steam demonstrated the excellent durability of these alloys under severe oxidizing conditions. The stainless steel– zirconium alloys immobilize and retain fission products very well and show potential for acceptance as high–level nuclear waste forms.

## ACKNOWLEDGMENTS

This work was supported by the U.S. Department of Energy, Nuclear Research and Development Program, under Contract No. W–31–109–ENG–38.

## REFERENCES

1. S. M. McDeavitt, D. P. Abraham, and J. Y. Park, J. Nucl. Mat. **257**, p. 21–34 (1998).
2. D.P. Abraham, S.M. McDeavitt, and J. Y. Park, Metall. Mater. Trans. **27A** p. 2151 (1996).
3. J. P. Ackerman, T. R. Johnson, L. S. H. Chow, E. L. Carls, W. H. Hannum, and J. J. Laidler, Prog. Nucl. Energy **31** p. 141 (1997).
4. D.P. Abraham, D. D. Keiser, Jr., and S.M. McDeavitt, Proc. Intl. Conf. on Decommissioning and Decontamination and on Nuclear and Hazardous Waste Management (SPECTRUM'98), Vol. 2, American Nuclear Society, LaGrange Park, IL p. 783 (1996).
5. D. A. Jones, *Principles and Prevention of Corrosion*, Macmillan Publishing, 1992, p. 145.
6. J. C. Farmer, R. D. McCright, A. K. Roy, G. E. Gdowski, F. T. Wang, J. C. Estill, K. J. King, S. R. Gordon, D. L. Fleming, and B. Y. Lum, Proc. 6th Intl. Conf. on Nucl. Eng., ICONE–6290, (1998).
7. A. E. Ogard and J. F. Kerrisk, LA–10188–MS, Los Alamos National Laboratory (1984).
8. J. K. Bates, M. G. Seitz, and M. J. Steindler, Nucl. and Chem. Waste Manag. **5** p. 63, (1984).
9. W. L. Ebert and J. K. Bates, Mater. Res. Soc. Symp. Proc. **176** , Pittsburgh, PA p. 339, (1990) 339.